

Emergency Soft Landing Trajectory Design for Multirotor Vehicles Under Rotor Failures

By Ye-ji HWANG,¹⁾ Ha-min JEON,¹⁾ Yeon-deuk JUNG,²⁾ Jong-han KIM¹⁾

¹⁾*Department of Aerospace Engineering, Inha University, Incheon, Republic of Korea*

²⁾*Unmanned Aircraft System Research Division, Korea Aerospace Research Institute, Daejeon, Republic of Korea*

Personal Air Vehicles (PAVs) are considered advantageous and promising for sustainable aviation, and the PAVs are being widely studied for academic research and commercialization purpose. Since the PAVs are expected to be operated mainly in highly populated urban areas, these malfunctions may cause severe property losses or even human casualties. For successful commercialization of the PAV industries, high reliable fault management techniques are essential to ensure the safety of the passengers, vehicles, and infrastructures. In this paper, we proposed an emergency landing trajectory replanning algorithm for rotor failure cases. And we verified the performance of the algorithm via a series of nonlinear 6-DOF simulations. As a result, it was shown that the proposed algorithm successfully generates the emergency landing trajectories under rotor failures. The fault tolerant control algorithm studied in this paper is expected to contribute to expanding the operational area of the urban air traffic system and enhancing stability.

Key Words: PAV(Personal Air Vehicle), UAM(Urban Air Mobility) Emergency Landing, Fault-Tolerant Control, Convex Optimization

Nomenclature

u, v, w	:	velocity at body frame
x, y, z	:	position at NED frame
I_x, I_y, I_z	:	moment of inertia
k_f	:	thrust coefficient
k_r	:	torque coefficient
g	:	gravity
m	:	mass of vehicle
Subscripts		
0	:	initial
f	:	final
b	:	body frame
n	:	NED frame
$c\theta$:	$\cos \theta$
$s\theta$:	$\sin \theta$

1. Introduction

Recently, due to the rapid increase of population in metropolitan area,¹⁾ where major infrastructures are highly concentrated, traffic congestion is getting worse due to the steady rise of the traffic volume and urban logistics from the spread of on-line shopping industries. Urban loops and intelligent transportation systems have been proposed to alleviate traffic congestion, but the ground transportation systems in many countries, including Korea, have been saturated by the rapid increase of the demands. As a result, there have been a lot of attempts to expand the industries to the sky, and Urban Air Mobility (UAM) is drawing a keen attention as a next-generation transportation.²⁾

Since the UAMs are expected to be operated in highly populated urban areas, their malfunctions may cause severe property losses or even human casualties.³⁾ For successful commercialization of the PAV industries, high reliable fault management

techniques are essential. In the case of multi-rotor vehicles, the dynamic responses under each rotor failure is different from that of the others, hence the analysis for the each rotor failure case and design of a real-time emergency landing algorithm for rotor failure cases are required..

In this paper, we proposed an emergency landing trajectory replanning algorithm for rotor failure cases. Based on the Finite Horizon Model Predictive Control (MPC) techniques, the proposed algorithm computes the minimum time soft landing trajectory and the guidance command under rotor failures. We verified the performance of the proposed algorithm via a series of nonlinear 6-DOF (6-Degree of Freedom) simulations. Numerical experiments with different emergency landing scenarios with a variety of state and control constraints were conducted.

2. Mathematical Model

2.1. Control Model

The vehicle used in this paper is shown in Figure 1. Propellers are attached to the leading edge and trailing edge of the wings, and the center of mass of the vehicle is located at the origin of the coordinate plane, also even-numbered propellers rotate counter-clockwise and odd-numbered propellers rotate clockwise. The aerodynamic forces generated by the main wings and the tail are neglected.

The state variables x, y, z are NED frame parameters with the starting point as the origin, and velocity variable u, v, w are body frame parameters. The following differential equation shows how the NED position is related to the body velocity.

$$\begin{bmatrix} \dot{x} \\ \dot{y} \\ \dot{z} \end{bmatrix} = C_b^n \begin{bmatrix} u \\ v \\ w \end{bmatrix}, \quad (1)$$

and the transformation matrix C_b^n can be described by euler an-

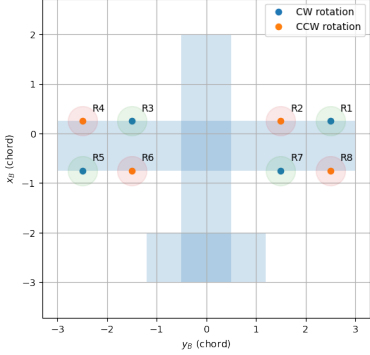


Fig. 1.: Diagram of the vehicle.

gles

$$C_b^n = \begin{bmatrix} c\psi c\theta & c\psi s\theta s\phi - s\psi c\phi & c\psi s\theta c\phi + s\psi s\phi \\ s\psi c\theta & s\psi s\theta s\phi + c\psi c\phi & s\psi s\theta c\phi - c\psi s\phi \\ -s\theta & c\theta s\phi & c\theta c\phi \end{bmatrix}, \quad (2)$$

where angular velocities are obtained as

$$\begin{bmatrix} p \\ q \\ r \end{bmatrix} = \begin{bmatrix} 1 & 0 & -s\theta \\ 0 & c\theta & s\phi c\theta \\ 0 & -s\phi & c\phi c\theta \end{bmatrix} \begin{bmatrix} \dot{\phi} \\ \dot{\theta} \\ \dot{\psi} \end{bmatrix}. \quad (3)$$

The translational dynamics in the body frame can be expressed as

$$\begin{aligned} \dot{u} &= -g \sin \theta - (qw - rv) \\ \dot{v} &= g \cos \theta \sin \phi - (ru - pw) \\ \dot{w} &= g \cos \theta \cos \phi - (pv - qu) - \frac{T}{m}, \end{aligned} \quad (4)$$

and the rotational dynamics are calculated by the following equations.

$$\begin{aligned} \dot{p} &= -\frac{I_z - I_y}{I_x} qr + \frac{\tau_\phi}{I_x} \\ \dot{q} &= -\frac{I_x - I_z}{I_y} rp + \frac{\tau_\theta}{I_y} \\ \dot{r} &= -\frac{I_y - I_x}{I_z} pq + \frac{\tau_\psi}{I_z} \end{aligned} \quad (5)$$

2.2. Rotor dynamics

The motion of multi-rotor aerial vehicles are controlled by summing up the downward thrust forces of the propellers and their induced reactive torques. Lift force of a rotor and its reactive torque produced by the actuators is described as Eq. (6).

$$f_i = \begin{bmatrix} 0 \\ 0 \\ k_f r_i^2 \end{bmatrix} \quad \tau_{f,i} = \begin{bmatrix} 0 \\ 0 \\ k_r r_i^2 \end{bmatrix} \quad (6)$$

The total thrust force and moment can be given as

$$T = \sum_{i=1}^n f_i \quad \tau = \sum_{i=1}^n (l_i \times f_i + \tau_{f,i}), \quad (7)$$

where i is the number of rotor.

2.3. Flight control system

The diagram of the designed flight control system is shown in Figure 2. The system is composed of horizontal position loop, altitude loop, attitude loop and mixer, that PD controller is introduced for all loops in it.

The rotor speed command can be calculated by Eq. (8). The classical mixer can be described as Eq. (8), and any right inverse matrix that satisfies Eq. (9) can be used for A^\dagger . The mixer was implemented by deriving a solution that minimizes the L2 norm of u , which can be calculated by multiplying the moore-penrose pseudo inverse on the desired control input.

$$A^\dagger c = u \quad (8)$$

$$AA^\dagger = I \quad (9)$$

In addition, the rotor is modeled by a simple secondary dynamics system, and the rotor speed command calculated from the mixer passes through a limiter that restricts to the motor output range. Also, slew rate, expressed as the change of the rotor speed, is limited as Eq. (10).

$$-\dot{r}_{\min} \leq \dot{r}_i \leq \dot{r}_{\max} \quad (10)$$

3. Emergency Soft Landing Trajectory Design

3.1. Problem

We proposed an emergency landing trajectory replanning algorithm for rotor failure cases. Based on MPC techniques, the proposed algorithm computes the minimum time soft landing trajectory and the guidance command under rotor failures. The optimal trajectory design problem of the algorithm can be described as follows,

$$\begin{aligned} &\text{minimize}_{T_c(t)} \quad \int_0^{t_f} \|T_c(t)\|^2 dt \\ &\text{subject to} \quad \ddot{r}(t) = g + \frac{T_c(t)}{m} \\ &\quad \|T_c(t)\| \leq \rho_1 \\ &\quad \dot{r}(0) = \dot{r}_0 \\ &\quad h(t_f) = \dot{r}(t_f) = 0 \\ &\quad \|T_c(t) - T_c(t-1)\| \leq \rho_2 \\ &\quad u_0^\top T_c(t) \geq \|u_0\| \|T_c(t)\| \cos \alpha_0, \end{aligned} \quad (11)$$

where

$$u_0 = \begin{bmatrix} 0 & 0 & -1 \end{bmatrix}^\top. \quad (12)$$

In Prob. (11), the designed problem tells it can derive an optimal thrust profile that minimizes total control efforts under the soft landing and kinematic constraints. The optimal profiles, attained by solving the problem with the initial state r_0, v_0 , should be less than maximum thrust ρ_1 . Also, to prevent maneuver instability, the thrust difference and the calculated thrust angle with respect to u_0 are limited to ρ_2 and α_0 on each. In particular, to increase landing stability, α_0 should become smaller for 0.5 seconds just before the landing.

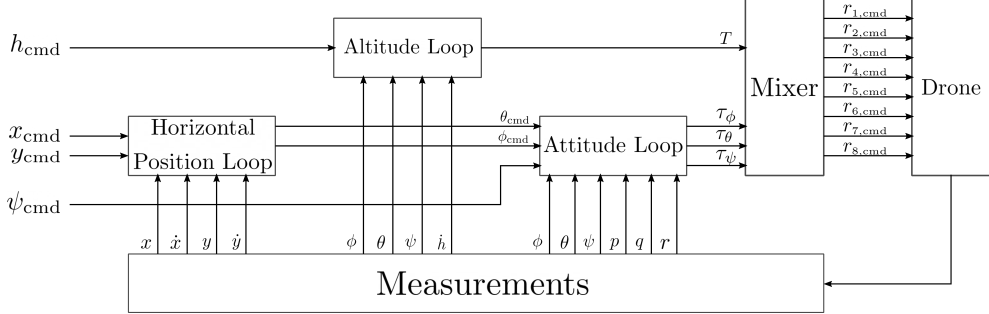


Fig. 2.: Flight control system.

3.2. Minimum time control

To optimize the flight time, find t that makes the problem Eq. (11) feasible through binary searching and generate the optimal trajectory. Following table is a pseudo code of binary search for optimal flight time.

Algorithm 1 Binary search for optimal flight time

```

1: Require:  $U, L, \epsilon$ 
2: while  $U - L > \epsilon$  do
3:    $t \leftarrow \frac{U+L}{2}$ 
4:   if problem at  $t_f = t$  is infeasible then
5:      $L \leftarrow t$ 
6:   else
7:      $U \leftarrow t$ 
8:   end if
9: end while
10:  $t_f \leftarrow U$ 
11: return  $t_f$ 
```

For the first iteration of the algorithm, the optimal landing trajectory is calculated for the given flight time $\frac{U+L}{2}$. At the given flight time, the lower bound will be set as $U+L/2$ if the optimal trajectory problem is infeasible, but the upper bound will become $\frac{U+L}{2}$ if it's feasible. After repeating the series of processes until $U - L$ is less than the stopping criterion (ϵ), the upper bound at the termination of the search is decided as the optimal flight time. From the designed trajectory with the optimal flight time t_f obtained by binary searching, we calculate the driving command of the vehicle. In Receding Horizon Control, only the command for the next control cycle is selected from the calculated profile, and applied to the 6-DOF simulator. Then, the induced state of the simulation will be a new initial condition for the next iteration of the trajectory replanning algorithm. After that, binary search is performed to derive t_f and calculate the optimal trajectory with the new initial states. Repeat this process until the vehicle lands on the ground to improve the robustness of the system.

3.3. Case study

To verify the designed soft landing algorithm, several experiments were performed in a 6-DOF simulation. Experiments were performed under different landing conditions, and the flight mission was set as shown in Table 1.

When performing the experiment, to simulate the failure situation, the rotation speed of the 6th rotor was set to 0 after 6 seconds from the beginning of the mission and the time required to detect the failure was assumed to be 0.2 seconds.

Table 1.: Flight mission

Time(s)	Altitude(m)	$x(m)$	$y(m)$	$\psi(\text{deg})$
0 ~ 3.5	4	3	2	10
3.5 ~ 6.2	4	5	6	10

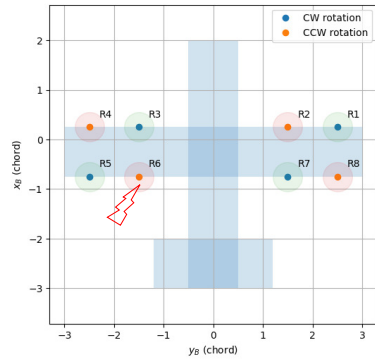


Fig. 3.: Faulty rotor.

Case 1

$$\text{Landing area constraint} \quad -\frac{1}{3}x + y \geq 0 \quad (13)$$

Case 2

$$\text{Landing area constraint} \quad \begin{cases} y \geq x - 2 \\ y \leq x + 3 \\ y \geq -2x + 10 \\ y \leq -3x + 20 \end{cases} \quad (14)$$

Case 3

$$\text{Landing area constraint} \quad (x - 3)^2 + (y - 3)^2 \leq \frac{1}{2} \quad (15)$$

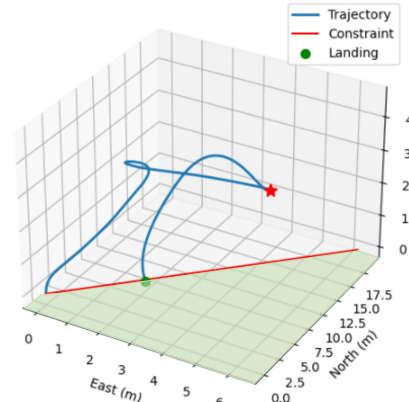


Fig. 4.: Trajectory of case 1. Failure occurs at star mark.

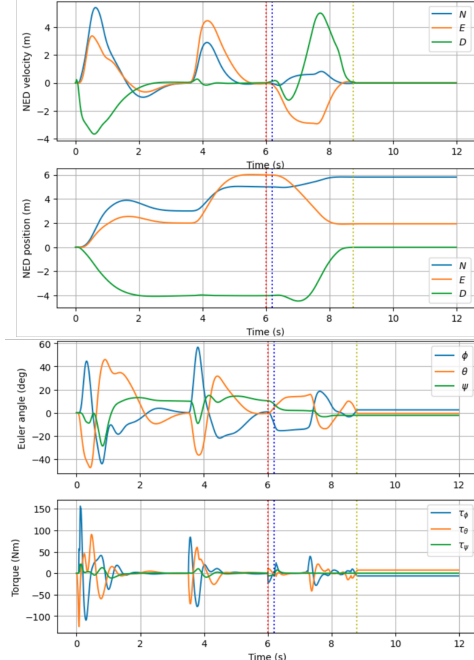


Fig. 5.: Euler angle, torque, and NED position result of case1.

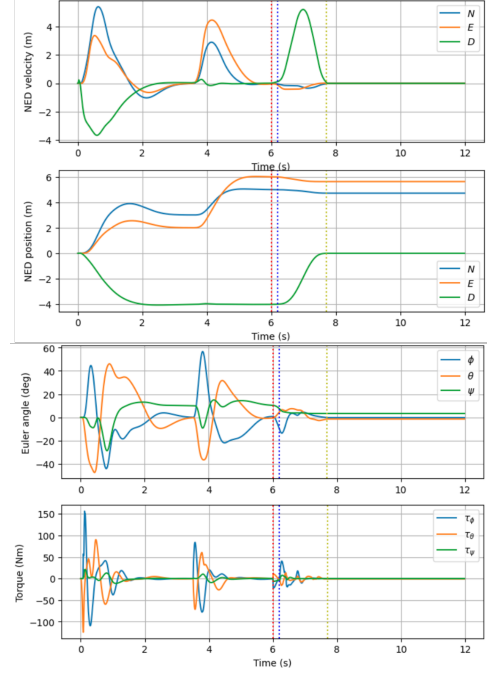


Fig. 8.: Euler angle, torque, and NED position result of case2.

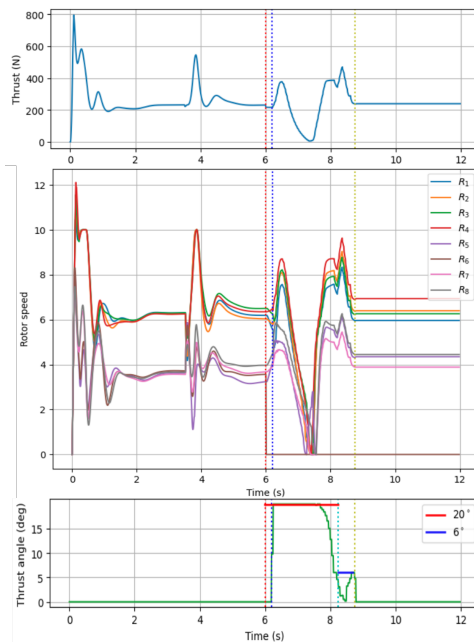


Fig. 6.: Thrust and rotor speed result of case1.

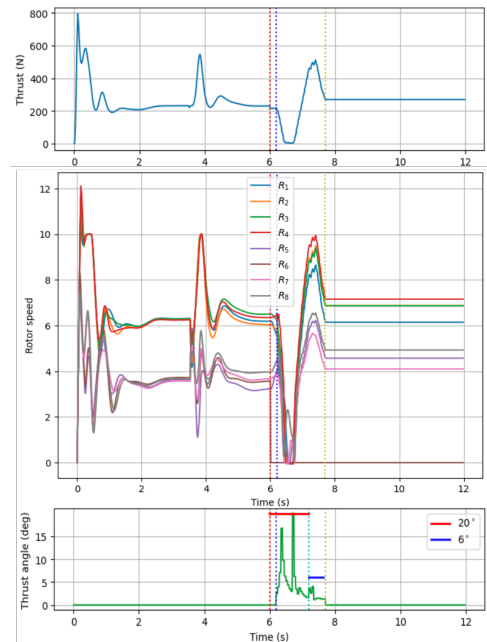


Fig. 9.: Thrust and rotor speed result of case2.

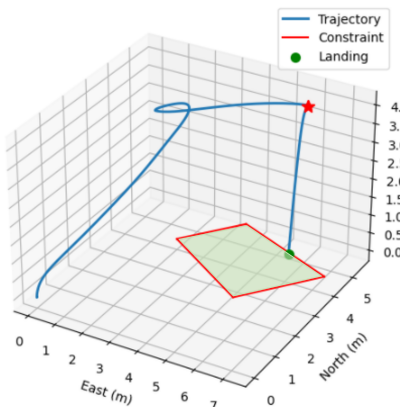


Fig. 7.: Trajectory of case 2. Failure occurs at star mark.

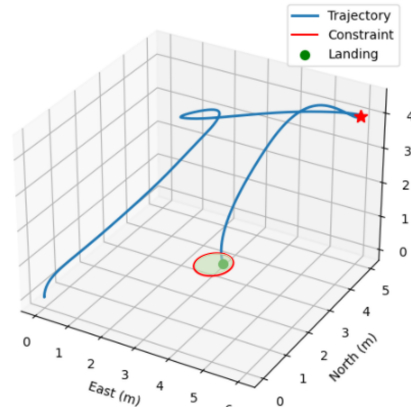


Fig. 10.: Trajectory of case 3. Failure occurs at star mark.

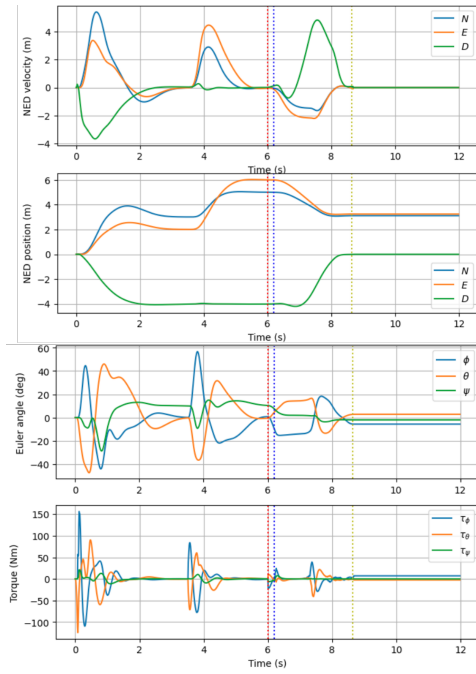


Fig. 11.: Euler angle, torque, and NED position result of case3.

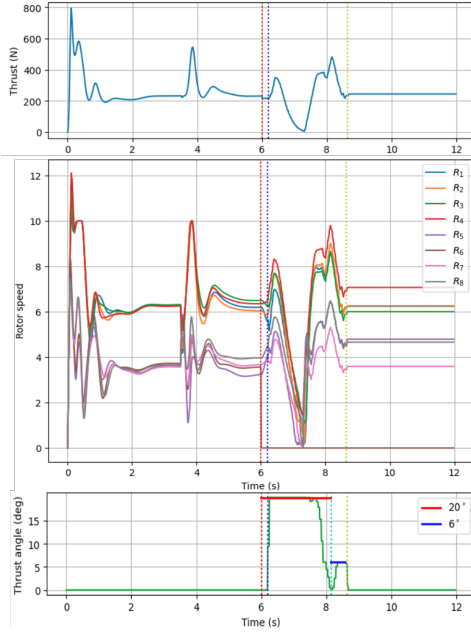


Fig. 12.: Thrust and rotor speed result of case3.

4. Conclusion

In this paper, we presented a trajectory replanning algorithm and an emergency landing guidance algorithm under rotor failures of a multi-propeller aircraft. The algorithm calculates the optimal landing trajectory and considers; 1)the thrust drop due to rotor failure, 2)the landing site constraint condition and 3)soft landing condition for an emergency situation.

We verified the performance of the proposed algorithm via a series of nonlinear 6-DOF simulations. Numerical experiments with different emergency landing cases with state and control constraints were conducted. As a result, it was shown that the proposed algorithm generates the emergency landing trajectories under rotor failures successfully.

Acknowledgments

This study was partially supported by the research project of “Study on the Core Technologies of Electric Vertical Take-Off & Landing Aircraft” funded by Korea Aerospace Research Institute. This work was also supported in part by INHA UNIVERSITY Research Grant.

References

- 1) CAFE FOUNDATION : Personal Air vehicle, (2015)
- 2) Parker D, Vascek and R. John Hansman : Scaling Constraints for Urban Air Mobility Operations: Air Traffic Control, Ground Infrastructure, and Noise, *AIAA J.*, (2018).
- 3) David P. Thippavong, Rafael D. Apaza, ryan E. Barmore : Urban Air Mobility Airspace Integration Concepts and Considerations, *AIAA J.*, (2018).